


RESEARCH

Open Access



Hybrid chitosan gold nanoparticles for photothermal therapy and enhanced cytotoxic action of 6-mercaptopurine on breast cancer cell line

Amna H. Faid^{1*} , Fatma El Zahraa Hussein², Elham M. Mostafa¹, Samia A. Shouman³, Yehia A. Badr¹ and Mahmoud A. Sliem^{1,4}

Abstract

Background One of the most popular anti-inflammatory and anti-leukemic medications is 6-mercaptopurine, along with its riboside derivatives. Because of their potent adverse effects and limited biological half-life, they are rarely used. These problems might be solved by a novel medication delivery technique based on gold nanoparticles (AuNPs). In present work, gold/chitosan nanohybrid was manufactured and assessed for photothermal therapy as well as a drug carrier to minimize the unwanted harmful effects of 6-Mercaptopurine (6-MP). We estimate loading of 6-MP on gold nanoparticles by chitosan reduction (Au@CS NPs) creating (Au@CS-6MP).

Results AuNPs were green sensitized in one step via chitosan. UV-visible spectroscopy, Zeta potential, TEM, FTIR spectroscopy, and HPLC technique for loading efficiency were used to characterize AuNPs and Au@CS-6MPC NPS. Our results estimate that AuNPs and Au@CS-6MPC NPS with small sizes of 16 ± 2 and 20 ± 4 nm, respectively, and Zeta potential 53.6 ± 5.2 and 55 ± 3 mV, respectively, and loading efficiency of 52% were achieved. Cytotoxicity of the Au@CS-6MPC NPs was significantly increased compared to free 6MP with IC_{50} 1.11 μ M. Cell viability was inhibited in AuNPs exposed to DPSS laser light, reaching 10% inhibition after 8 min.

Conclusions The prepared Au@CS-6MPC NPs resulted in an additive effect in therapeutic managing of breast cancer. It can be predicted that this nanocomposite along with synergistic effect of laser light will definitely result in better therapeutic efficacy and reduced side effects of 6-MP in a combination photothermal chemotherapy treatment. This combination can be explored as future alternative for cancer therapy.

Keywords Green synthesis, Gold nanoparticles, Cytotoxicity, Drug delivery, Photothermal therapy

1 Background

Despite the incredible progress made in medication over the past few years, Cancer continues to be a significant worldwide health issue, responsible for over 10 million deaths in 2018. Breast cancer is caused by the uncontrolled growth of breast cells. According to the World Health Organization, breast cancer was the greatest common cancer globally in 2021. Statistics have shown that one in eight US women develops breast cancer [1]. The most difficult aspects of cancer

*Correspondence:

Amna H. Faid

amna.hussein@cu.edu.eg

¹ National Institute of Laser Enhanced Science, Cairo University, Giza, Egypt

² Faculty of Engineering, Helwan University, 11795 Cairo, Egypt

³ Cancer Biology, National Cancer Institute (NCI), Cairo University, Giza, Egypt

⁴ Chemistry Department, Faculty of Science and Arts, Taibah University, 100823 Al-Ula, Saudi Arabia



© The Author(s) 2023. **Open Access** This article is licensed under a Creative Commons Attribution 4.0 International License, which permits use, sharing, adaptation, distribution and reproduction in any medium or format, as long as you give appropriate credit to the original author(s) and the source, provide a link to the Creative Commons licence, and indicate if changes were made. The images or other third party material in this article are included in the article's Creative Commons licence, unless indicated otherwise in a credit line to the material. If material is not included in the article's Creative Commons licence and your intended use is not permitted by statutory regulation or exceeds the permitted use, you will need to obtain permission directly from the copyright holder. To view a copy of this licence, visit <http://creativecommons.org/licenses/by/4.0/>.

treatment are drug resistance that the body develops and damage caused by the drug to non-malignant cells [2]. In recent years, there has been a rise in the research into nanotechnology across a wide range of fields, including biomedicine, where nanoparticles have been assessed for their ability to treat various diseases like cancer. An intriguing possibility for cancer diagnostics and treatment has emerged [3]. Optical, electrical, mechanical, and biological properties of metal nanoparticles are distinctive. In this line, there have recently been more reports on polymer-metal nanocomposites. There are abundant green and sustainable methods for manufacturing NPs, including microorganisms (bacteria, fungi, and yeast), biomolecules, and plants. Greener methods to synthesizing biogenic NPs are constantly in request by researchers to diminish toxic effects and maintain a green environment because of their biocompatible, clean, cost-effective, and eco-friendly properties [4]. Metallic nanoparticles specially gold nanoparticles (AuNPs), one of several kinds of nanoparticles, have been found to suppress growth and trigger cell death in a variety of biological systems [5–8]. AuNPs are biocompatible and have a strong affinity for biomolecules holding amines, disulphide bonds, and thiol groups. Compounds containing these moieties can be simply loaded onto the surface of AuNPs. Nitrogenous-based derivatives such as 6-mercaptopurine (6-MP) and 6-thioguanine (6-TG) [9]. For the creation of nanocomposites for particular purposes, AuNPs are produced from a range of polymer matrices such as chitosan (CS) [10, 11]. A derivative of chitin, chitosan (CS), is found in the cell walls of fungus and yeast as well as the exoskeleton of arthropods [12]. Chitosan's cationic character is primarily responsible for the electrostatic interaction with metal nanoparticles, and it can be used to reduce and stabilize gold, generating zero-valent nanoparticles in the process. Additionally, it offers enough charge via the amino groups, aiding in the attachment of the biomolecules in the future, ensuring optimal stability, and enhancing the uptake of the nanoparticles [13]. Amongst newly developed cancer treatments, photothermal therapy (PTT) uses the photothermal action of photothermal agents (PTAs) to heat up absorbed light energy and burn tumours, owing to its easy use, speedy recovery, and brief therapy. PTT is highly valuable for research and can raise the temperature of some tissues [14]. PTT specifically kills cancer cells that are more susceptible to high temperatures. In addition to surface plasmon resonance (SPR), AuNPs have distinctive physico-chemical characteristics that depend on the interaction between electromagnetic waves and free electrons in the AuNPs surface's conduction band, leading to their

coherent resonant vibrations at frequencies associated with visible light. This process makes gold nanoparticles more effective in scattering and absorbing light, which is helpful for a number of biomedical applications [15]. Additionally, AuNPs have been thought of as a photothermal agent, able to transform electromagnetic radiation into thermal energy through electronic excitation and relaxation. For biomedical applications, spherical gold nanoparticles with sizes of 10–30 nm work well as photothermal agents [16]. As a result, utilizing gold nanoparticles as photothermal agents is an effective technique to cause precise heating that can kill cancerous cells with little harm to other tissues. Some reports claim that their anticancer activity is due to enhanced apoptosis in cancer, cells through cell cycle arrest in addition to activation of ROS and caspase-3 mediated signalling. Lastly, in cancerous cells, they cause mitochondrial depolarization and DNA damage [17]. For the treatment of inflammatory conditions, acute lymphoblastic leukaemia, acute myelocytic leukaemia, and acute lymphoblastic leukaemia 6-MP were used. 6-MP is one of the most efficient anticancer medications. Due to 6-MP's unfortunate bioavailability and brief plasma half-life, its application is restricted [18]. Due to 6-MP's unfortunate bioavailability and short-term plasma half-life, its application is constrained. Infection, allergic reactions, pancreatitis, hepatotoxicity, and myelosuppression resulting in anaemia, a low white blood cell count, and/or a low platelet count are all risks that are increased. As a result, numerous tailored drug carriers have been created to improve the effectiveness of currently available therapies, guard the drug against biodegradation before it reaches the target cells, and lessen anticipated side effects.

Here, we deal with biosynthesis of AuNPs by means of chitosan for MP delivery forming 6MP-AuNPs nanocomposite. Additionally, nanocomposite's cytotoxic effects and PTT on MCF7 were carried out.

2 Methods

2.1 Materials

All chemicals used in the preparation and investigation of the present study were of highest available purity and used as received without any purification. Tetrachloroauric acid ($\text{HAuCl}_4 \cdot 3\text{H}_2\text{O}$), 6-mercaptopurine (6-MP), Chitosan low molecular weight, Dimethylsulphoxide (DMSO), RPMI-1640 medium, Sodium bicarbonate (Sigma Chemical, Trypan blue, Foetal Bovine Serum (FBS), Penicillin/Streptomycin, Trypsin, Acetic acid. Sulphorhodamine-B (SRB), Trichloroacetic acid (TCA), and Tris base are obtained from Sigma Aldrich Chemical Co., St. Louis, Mo, USA.

2.2 Preparation of chitosan reduced gold nanoparticles (AuNPs) and Au@CS-6MPC NPs

Chitosan was used for the creation of the Au@CS NPs, 100 mL of chitosan solution containing 1% acetic acid was first created, heated on a hot plate to boiling, and then 100 mL of $\text{HAuCl}_4 \cdot 3\text{H}_2\text{O}$ solution was added. This mixture was then heated at 100 °C for 15 min while being constantly stirred to generate a red colour [19]. Furthermore, Au@CS-6MPC NPs were created by coating Au@CS NPs with 6MP. Various concentrations of 6MP (0.00125, 0.0025, 0.005, 0.01, and 0.02 mM) were mixed dropwise with 1 mL of the synthesised AuNPs and sonicated for 20 min.

2.3 Determination of potential cytotoxicity of 6MP and Au@CS-6MPC NPs on MCF7 cell line

Different concentrations of 6MP and Au@CS-6MPC NPs were used. The American Type Culture Collection (ATCC, Minnesota, USA) provided the MCF7 cell line. The tumour cell line was kept at National Cancer Institute (NCI), Cairo, Egypt. The antitumour activities of nanomaterials assessed by the sulphorhodamine-B (SRB) assay according to Skehan [20]. Briefly, cells were seeded at a density of 3×10^3 cells/well in 96-well microtiter plates. Then left to attach for 24 h before incubation with drugs. Subsequently, cells were treated with different concentrations of 6MP and Au@CS-6MPC NPs (1.25, 2.5, 5, 10, and 20 μM), three wells were used and incubation was continued for 48 h. DMSO was used as a control (1% v/v). At the end of incubation, cells were fixed with 20% trichloroacetic acid and stained with 0.4% SRB dye. The optical density (OD) of each well was measured spectrophotometrically at 570 nm using ELISA microplate reader (TECAN sunrise™, Germany). The mean survival fraction was calculated as follows: O.D. of the treated cells/O.D. of the control cells. The IC₅₀ (concentration that produces 50% of cell growth inhibition) value of each drug was calculated using sigmoidal dose-response curve-fitting models.

2.4 Photothermal therapy (laser toxicity)

A second harmonic Nd:YAG DPSS laser with a 150 mW wavelength at 532 nm was employed to emit laser light. Exactly as previously mentioned, cells were planted. The cells were treated with 125 L/mL of AuNPs, allowed to sit for 48 h, and then subjected to laser light for 2, 4, 6, and 8 min, respectively. To examine the impact of laser light on the cells (light control), cells without nanoparticles were exposed to laser light for the same amount of time. Cells were fixed and examined when the exposure period was complete.

2.5 Characterization techniques

2.5.1 UV-visible absorption spectroscopy

Absorption spectra of the synthesized chitosan stabilized Au@CS NPs and Au@CS-6MPC NPs were evaluated using a double beam spectrophotometer (PG instrument, T80+, UK.). In order to record the absorbance within the proper scan range (200–800 nm), 200 μL from the produced solutions were poured in a 1 cm UV-quartz and diluted to 2 mL with pure water.

2.5.2 Transmission electron microscopy (TEM)

TEM was used by the Nanotechnology and Advanced Material Central Lab (NAMCL), Agriculture Research Centre (ARC), to examine the morphology of Au@CS NPs and Au@CS-6MPC NPs. Dutch company FEI is its name. Tecnai G20 model, Super twin, double tilt, and Magnification range of up to 1,000,000 \times , 200 kV applied voltage, and LaB₆ gun type.

2.5.3 Particle size and zeta potential

By measuring zeta potential without dilution, the surface charges and particle size of Au@CS NPs and Au@CS-6MPC NPs were determined based on photon correlation spectroscopy, the zeta potential and particle size was calculated using the Zetasizer 300 HAS (Malvern Instruments, Malvern, UK) Analysis. Analysis time was 60 s.

2.5.4 Fourier transform infrared spectroscopy (FTIRs)

FTIR measurements were made between 500 and 4500 cm^{-1} using an FTIR spectrometer (4100 Jasco-Japan). Using a lyophilizer, prepared samples (free 6-MP and Au@CS-6MPC NPs) were freeze-dried. Potassium bromide (KBr) pellet was used to dilute the IR spectra of the powdered materials.

2.5.5 HPLC analysis

The loading efficiency of 6MP on Au@CS NPs was assessed using a high-performance liquid chromatography HPLC, As mentioned previous, selection of the mobile phase was based on the polarity of the sample, availability of the solvents, proper retention time (RT), the sensitivity of the assay, and a short run time of the sample. HPLC Chromatograph YL-9100 system with C-18 (250 mm \times 4.6 mm \times 5 μm). The mobile phase used was acetonitrile and 0.05 M sodium acetate buffer in the ratio 10:90 with pH adjusted to 6.8 using HPLC grade glacial acetic acid at a flow rate of 1 mL/min. Wavelength was fixed at 324 nm. Analyses were performed at Micro Analytical Center, Cairo University, Giza Governorate, Egypt. The pure 6-MP standard curve was developed, and the unbound drug was

computed using the standard curve. The loading percentage was determined by the following formula:

$$\frac{(\text{Total 6 MP} - \text{free 6 MP})}{\text{Total 6 MP}} \times 100$$

2.5.6 Enzyme-linked immunosorbent assay (ELISA)

ELISA (also known as Microplate Readers) is a group of laboratory instruments designed to detect biological, chemical or physical events of samples in microtiter plates. The most common microplate format used in academic research laboratories or clinical diagnostic laboratories is 96-well (8 by 12 matrix) with a typical

reaction volume between 100 and 200 μL per well. The ELISA reader used in our measurements is ELISA microplate reader (Meter tech. Σ 960, USA.).

2.6 Statistical analysis

The arithmetic mean SD is used to express data. The San Diego, USA-based GraphPad Software Prism v5 was used for the statistical analysis. The findings from the transfection assay were statistically analysed using the Tukey multiple comparison test and a single pooled variance. When $p < 0.05$, differences were deemed statistically significant.

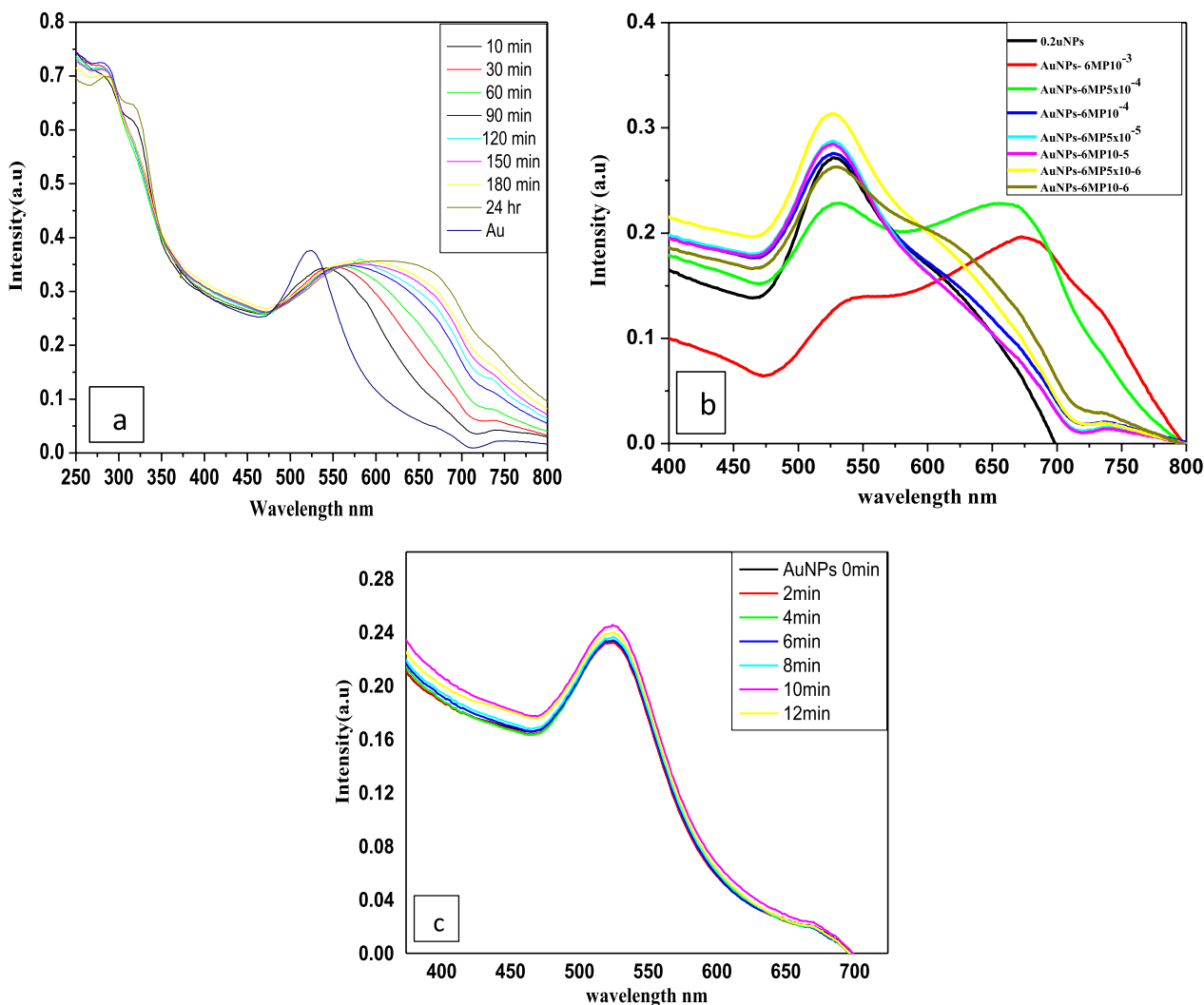


Fig. 1 UV-visible spectrum of **a** AuNPs and 1 mM Au@CS-6MPC NPs at different time intervals, **b** Au@CS-6MPC NPs at different 6-MP concentrations, and **c** AuNPs at different time intervals of exposure DPSS laser irradiation

3 Results

At 523 nm, AuNPs exhibit the surface Plasmon band SPB. Figure 1a and b, which displays the absorption spectra of AuNPs and Au@CS-6MPC NPs, illustrates UV–visible spectroscopy used to examine the interaction between 6-MP and Au@CSNPs. The band in the UV region of 6-MP developed at 321 nm climbing from the $n-\pi^*$ transition of the 6MP molecule [21]. There were a decrease in absorption band of 6-MP after loading on AuNPs.

3.1 Factors affecting the formation of Au@CS-6MPC NPs

By observing the changes in the AuNPs’ absorption spectra after the addition of 6-MP at various time intervals, it was possible to ascertain how time affected the interaction between 6-MP and AuNPs. The plasmon band of AuNPs widened after 10 min, as depicted in Fig. 1a. The solution’s colour changed from wine red to violet. After 150 min at 650 nm, a new broad peak begins to emerge clearly with a startling increase in intensity over time. We further investigated the effect of different 6-MP concentrations on AuNPs loading by recording the absorption band. Figure 1b represents the absorption spectra of the resulting solutions measured after 24 h of mixing. As clearly observed, there is a broadening of the SPR band of AuNPs. Alternatively, the solutions containing high concentrations of the drug showed a more complex assembly of AuNPs as their absorption spectra show broadband at a higher wavelength assigned to the plasmonic coupling. The produced AuNPs absorption spectra were measured after laser irradiation to study the influence of laser irradiation with various irradiation time intervals and show high stability as there is no change in absorption peak Fig. 1c.

Figure 2a and b show TEM images of Au@CSNPs and Au@CS-6MPC NPs, which demonstrate that the

Table 1 Zeta potential of Au@CS NPs and Au@CS-6MPC NPs

| | Zeta potential | PDI |
|----------------|----------------|-------|
| Au@CS NPs | 53.6 ± 5.2 | 0.324 |
| Au@CS-6MPC NPs | 55 ± 3 | 0.72 |

nanocomposite had a consistently spherical form with uniform size distribution and a smooth surface with slight increase in particle size after 6-MP loading as the particle size increased from 16 ± 2 to 20 ± 4 nm.

According to Table 1 and Fig. 3a, the zeta potential of Au@CSNPs and Au@CS-6MPC NPs were examined. The higher the zeta potential, the more stable the nanoparticles are due to a larger repulsive force between them. Additionally, nanoparticle charge density has a significant impact on how well they adhere to the negatively charged cancer cell membrane. In order to develop drug delivery carriers for the treatment of cancer, positively charged nanoparticles are recommended. Electrostatic repulsions frequently make charged particles with an ideal zeta potential ≥ 30 mV less likely to aggregate [21]. AuNPs that had been prepared by CS displayed a high zeta potential along with small, uniformly sized particles. The long-term stability and cellular behaviour for drug release were measured by studying zeta potential as a function of surface charge of particles. AuNPs and 6MP/AuNPs NC have zeta potentials 53.6 ± 5.2 to 55 ± 3 mV, respectively, which indicate the high stability of AuNPs and 6MP/AuNPs NC.

FTIR experiments were used to confirm the binding interaction of 6-MP loaded AuNPs. Figure 4 and Table 2 display the FTIR spectra of 6-MP and Au@CS-6MPC NPs, respectively. AuNPs have an attractive applicant in cancer therapy and appear to provide a flexible platform

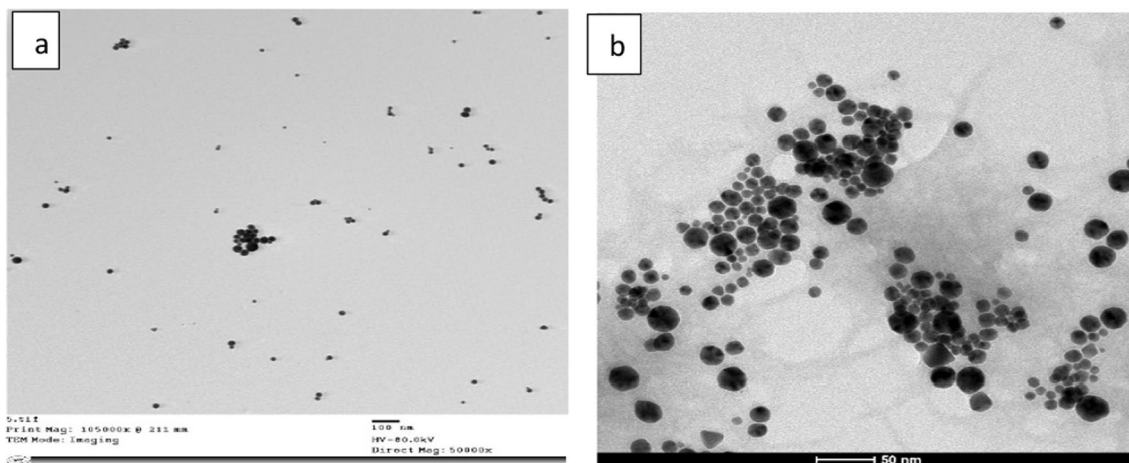


Fig. 2 TEM images of **a** Au@CSNPs and **b** Au@CS-6MPC NPs

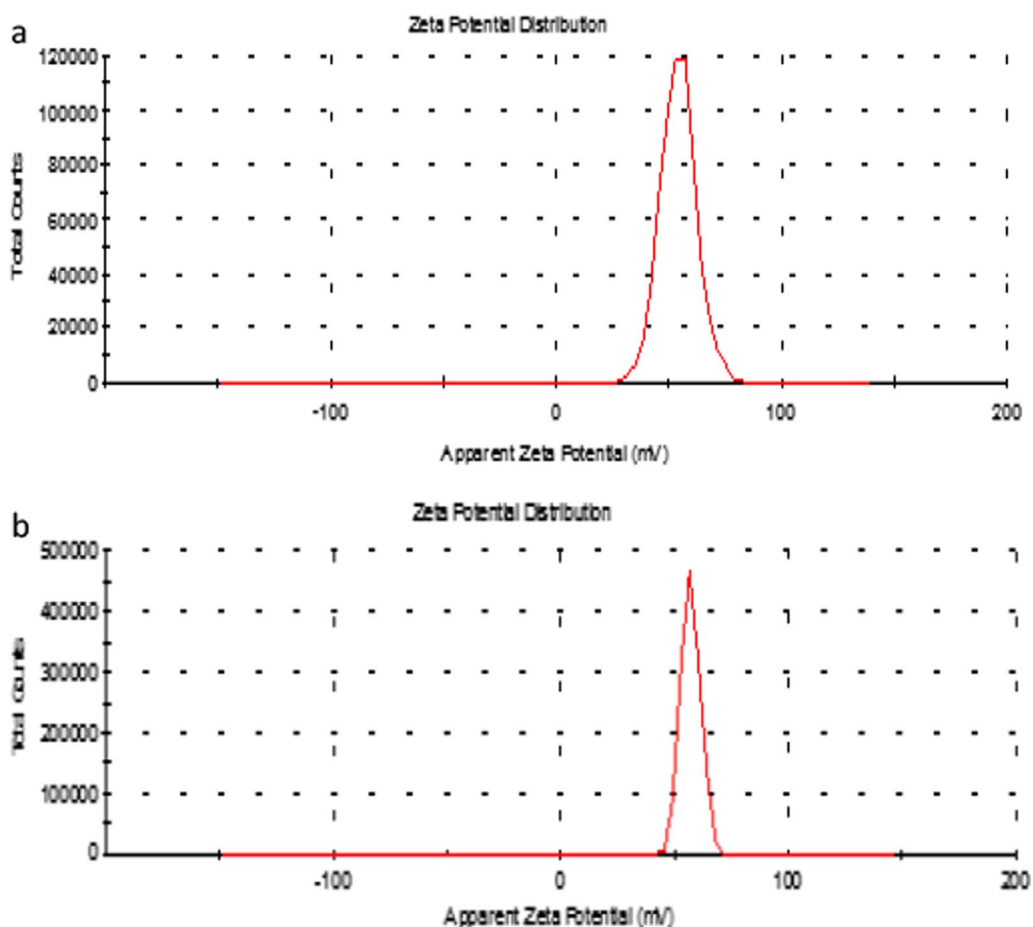


Fig. 3 Zeta potential for **a** chitosan reduced AuNPs and **b** AuNPs /6MPNC

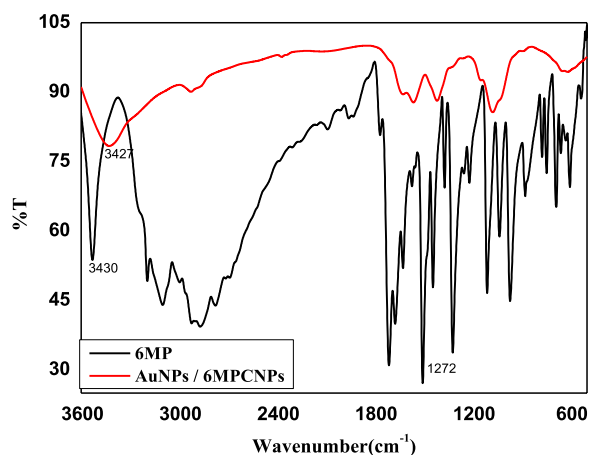


Fig. 4 FTIR spectra of 6-MP and Au@CS-6MPC NPs

Table 2 FTIR spectra of 6-MP and Au@CS-6MPC NPs presented in Fig. 4 [23]

| Fundamental vibrations | Frequency (cm^{-1}) |
|--|--------------------------------|
| <i>6MP</i> | |
| The combined stretching vibration peak of the NH_2 and OH group | 3430.74 |
| C–H (stretch) | 3094.23 |
| N–H (Bend) | 1527.35 |
| C–N ring vibration | 2999.73 |
| C=N ring vibration | 1344.14 |
| C=C ring vibration | 1613.16 |
| $\nu_{\text{C}=\text{S}}$ /ring vibration | 1668.12 |
| C=S stretching | 1272.79 |
| $\nu_{\text{C}=\text{S}}$ /ring vibration | 1154.19 |
| <i>Au@CS-6MPC NPs</i> | |
| Combined stretching vibration NH_2 and OH group | 3427 |
| $\nu_{\text{C}=\text{S}}$ /ring vibration | 1154.19 |

for the delivery of drugs with thiol functionalities. The drugs bearing sulphur groups on their structures reveal strong affinity for binding to AuNPs. In the solid state,

6-MP occurs as a tautomeric form (with a C=S group) and its IR spectrum displays the corresponding absorption characteristic bands at 3430.74, 1527.35, 3094.23, 2999.73, 1344.14, 1613.16, 1668.12, 2676.71, 1154.19, 1120.44 and 1272.79 cm^{-1} corresponding to combined peaks of the NH_2 and OH group stretching vibration, N-H (Bend), C-H(stretch), C-N, C=N, C=C, $\nu\text{C}=\text{S}$ /ring vibration, $\nu\text{C}=\text{S}$ /ring vibration and C=S stretching, respectively [22]. The intensity of all bands decreased when Au@CS-6MPC NPs were loaded, and the peak at 3430 cm^{-1} was extended and slightly displaced to lower wavelengths at 3427 cm^{-1} indicating the creation of composite Au@CS-6MPC NPs.

The loading efficiency was measured by HPLC as shown in Fig. 5a and b, respectively; 6-MP exhibits band at a retention time of 3.8 min. The loading efficiency was found to be 52%.

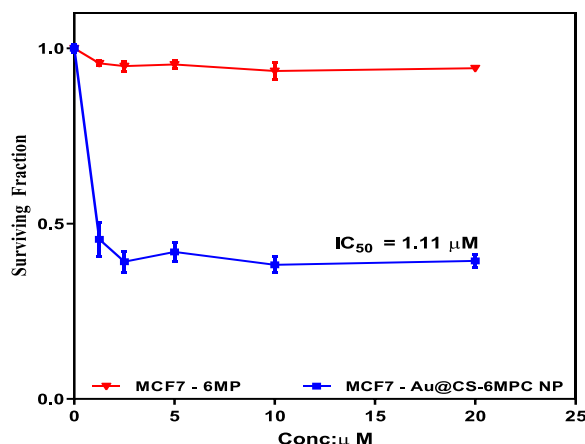


Fig. 6 Cytotoxicity of different concentrations of 6-MP and Au@CS-6MPC NPs on MCF7 cell line after 48 h

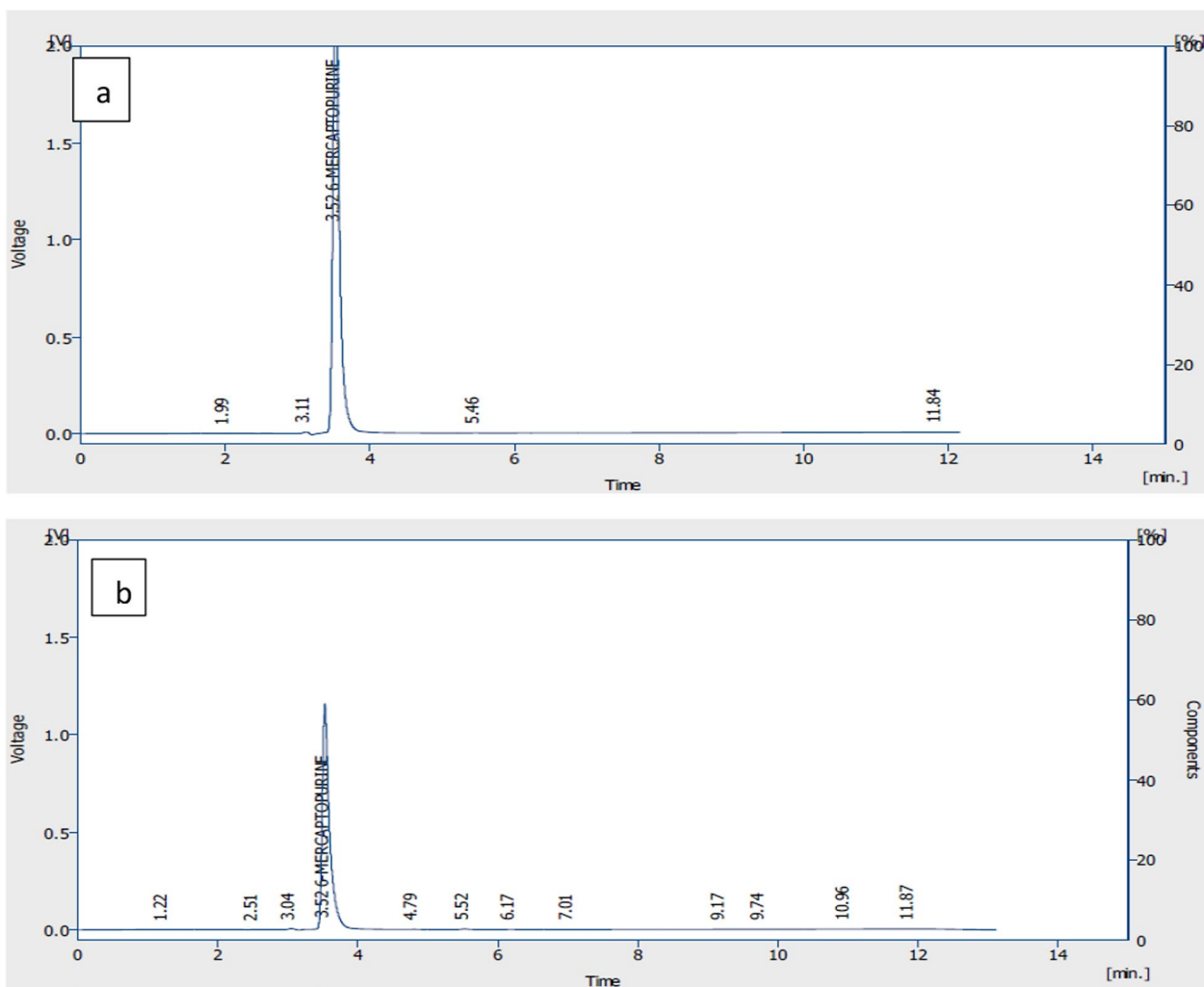


Fig. 5 HPLC for a 6-MP and b 6-MP/AuNPs NC

3.2 Anticancer efficiency of 6-MP and Au@CS-6MPC NPs on MCF7

Figure 6 shows cytotoxic effect of various concentrations (1.25, 2.5, 5, 10, and 20 μM) of 6-MP and Au@CS-6MPC NPs on breast cancer cell line (MCF7) after 48 h. A decrease in cellular propagation was seen when the drug concentration was increased. 6-MP produced a 7% lessening in cell survival at 10 μM , while Au@CS-6MPC NPs produced a decline in cell viability reaching maximum cytotoxicity 62% at 10 μM compared to the control with IC50 1.11 μM .

3.3 Photothermal therapy on MCF7 cell line

In order to confirm that photothermal results were exclusively achieved as a result of the laser activation of AuNPs, as shown in Fig. 7, the laser control experiment was carried out to assess the impact of DPSS laser on MCF7 cell line viability in the absence of the nanoparticles. A 532 nm, 150 mW DPSS laser was used to treat MCF7 tumour cells at various intervals (2, 4, 6, and 8 min).

4 Discussion

After adding 6-MP to AuNPs, the absorbance spectra revealed a slight red shift from 523 to 529 nm along with a drop in absorbance strength. This little modification is due to the particle size growing after loading. At 670 nm, a higher wavelength, another new band was discovered. As a result of the 6-MP addition, which results in interparticle interaction between the nearby AuNPs, this band is present. A colour change from red to mauve can be used to demonstrate the accumulation of gold nanoparticles by adding 6-MP to AuNPs and slightly growing their size [24].

The disappearance of a distinctive 6-MP peak at 1272 cm^{-1} equivalent to C=S stretching approving the presence of complex formation of the 6-MP with AuNPs through the sulphur atom, while there were no changes

to -NH or C-N stretching frequencies demonstrating that these groups are not involved in binding with AuNPs. The drugs bearing sulphur groups on their structures exhibit a strong affinity for binding to AuNPs. From the above data, it is apparent that the binding of 6-MP with AuNPs occurs through the sulphur atom [14]. HPLC system was used to determine the drug loading efficacy of the nanocomposite. First a standard calibration curve of 6-mercaptopurine was done. Then, the supernatant collected from the purification of the nanocomposite by centrifugation was assayed for 6-mercaptopurine by the same system. The concentration of 6-MP in supernatant was determined by measuring its area under peak as a mean of three independent injections of the sample then using the standard curve to define the corresponding concentration. In the case of Au@CS-6MPC NPs, the band intensity decreases which may be as a result of a reduction in drug concentration confirming loading of 6-MP on the AuNPs surface.

Due to focused delivery, Au@CS6MPC NPs may accumulate better by an endocytosis mechanism at their site of action, thereby increasing their cytotoxicity. Compared to free medications, nanoparticles are frequently nonspecifically internalised into cells through endocytosis or phagocytosis. The sources of the positive charges on the Au@CS6MPC NPs' surfaces are the adsorbed positive Au ions, which greatly aids their ability to pass through the negatively charged cancer cell membranes [3, 25]; therefore, the electrostatic interaction might facilitate MCF7 cancer cells' uptake of Au@CS6MPC NPs. Since many biological things at the nanoscale, including proteins, viruses, and fragments of other cells, are intrinsically similar to nanoparticles, their endocytosis can be transmitted to the lysosomes for digestion. Similar to free 6-MP, Au@CS-6MPC NPs can be taken up by the MCF7 cell line, which then transports them to a lysosome where the thiol group is protonated and the Au-S bond is broken, releasing the free drug, which then diffuses through the cell like free 6-MP [26]. Overall, increased intracellular absorption of the functionalized AuNPs and subsequent release in lysosomes are responsible for Au@CS-6MPC NPs' improved anti-proliferation compared to 6-MP. According to their research, Aghevlian et al. 2012 found that on MCF7 cells at concentrations of 12.5 M, 6-Thioguanine (6TG) loaded AuNPs considerably outperformed free 6-Thioguanine (6TG) in terms of anti-proliferation activity. Increasing exposure time, the less the average survival rate. The marginally reduced survival rate with increasing exposure light dose suggests that laser has a marginally cytotoxic effect on the MCF7 cell line. However, the cytotoxic effect of light has a negligibly little impact on cell death. The minor decline in cell viability may be intended to draw attention to the damage

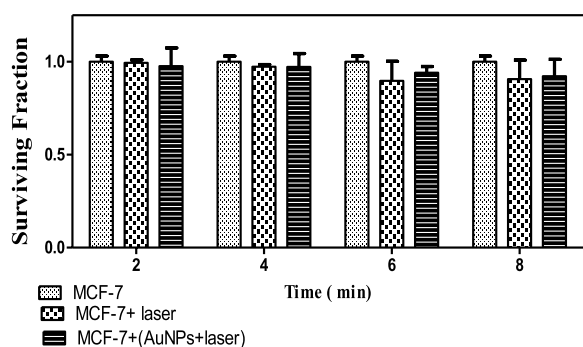


Fig. 7 The effect of DPSS laser irradiation on the viability of MCF7 and MCF7 incubated with Au@CS NPs

that heat shock does to cell membrane integrity, which worsens permeability [27–29]. The tumour environment is more acidic, nutrient deficient, and hypoxic than that of regular tissues, which makes it more sensitive to heat. Since cells are thermosensitive and their membranes should experience permeability changes at this temperature [30]. Figure 7 depicts measurements of cell viability after 48 h of incubation, which revealed a small decline with a maximum 10% inhibition after 8 min. The results revealed a steady decline in cell viability with increasing laser exposure time; this finding may be explained by the fact that spherical AuNPs with diameters between 10 and 30 nm are appropriate photothermal agents for biomedical applications because they have a high photothermal conductivity. Due to electron–phonon and phonon–phonon processes, they have been found to be non-toxic and to exhibit a distinctive localized SPB band approximately 520 nm with an effective light-to-heat conversion on a picosecond time scale. As a result, when exposed to laser light at the surface plasmon absorption band, the nanoparticles quickly convert the photon energy they have just absorbed into heat energy [31]. Then, on a timescale of around 100 ps, the lattice of the nanoparticles rapidly cools by exchanging energy with the surroundings. As a result, using AuNPs as photothermal agents is an effective technique to provide precise heating while causing less harm to nearby tissues and harming malignant cells, which are more susceptible to heat.

Our results were in agreement with Rita Mendes et al. [32]; using breast cancer as a model, they demonstrate the effective light to heat conversion of spherical 14 nm AuNPs prepared by chemical means and irradiated using a continuous wave (CW) 532 nm green diode-pumped solid-state laser (DPSS). Their results indicate that the irradiation of cells in the presence of AuNPs results in greater inhibition than in the absence of nanoparticles.

5 Conclusion

It is worth noting that resistance to chemotherapy limits the effectiveness of anticancer drug treatment. Overcoming this limitation can change the survival of cancer. In this work, a technique for producing AuNPs utilizing the biocompatible polymer chitosan that is quick, environmentally friendly, highly stable, and inexpensive. The produced AuNPs is spherical shape with a high degree of stability. When exposed to a visible DPSS laser, Au@CS NPs are used as photothermal agents with effective light-to-heat conversion. The generated Au@CS NPs were also employed as carriers for the anticancer 6-MP to create Au@CS6MPC NPs, which significantly reduce the survival of the breast cell line MCF7 and have an IC₅₀ of 1.11 M. Further research and investigation are required to discover these compounds' full potential on different

cell lines and underlying mechanisms for developing novel therapeutic drugs.

Acknowledgements

Not applicable.

Authors' contributions

AHF conceived the research idea, prepared samples, conducted UV-VIS, FTIR measurements and analyzed data with assistance from MAS, YAB, EMM, FEH, SAS and AHF performed cytotoxicity experiments and analyzed the experimental data. AHF wrote the manuscript and designed the figures, with technical input from EMM. Collectively, the authors assisted in the data analysis and technical discussion. All authors read and approved the final manuscript.

Funding

This research did not receive any specific grant from funding agencies in the public, commercial, or not-for-profit sectors.

Availability of data and materials

The datasets used and/or analysed during the current study are available from the corresponding author on reasonable request.

Declarations

Ethics approval and consent to participate

Ethics committee name: National Institute of Laser Enhanced Science Cairo University, NILES Ethics Committee. Approval reference: NILES-EC-CU 23/8/18. Written consent is not required.

Consent for publication

Not applicable.

Competing interests

The authors declare that they have no competing interests.

Received: 5 June 2023 Accepted: 29 August 2023

Published online: 14 September 2023

References

- McGuire S (2016) World cancer report 2014. Geneva, Switzerland: World Health Organization, International Agency for Research on Cancer, WHO Press, 2015. *Adv Nutr* 7(2):418–419
- Yafout M, Ousaid A, Khayati Y et al (2021) Gold nanoparticles as a drug delivery system for standard chemotherapeutics: a new lead for targeted pharmacological cancer treatments. *Sci Afr* 11:e00685
- Nour M, Hamdy O, Faid AH et al (2022) Utilization of gold nanoparticles for the detection of squamous cell carcinoma of the tongue based on laser-induced fluorescence and diffuse reflectance characteristics: an in vitro study. *Lasers Med Sci* 37(9):3551–3560
- Khan MF, Khan MA (2023) Plant-derived metal nanoparticles (PDMNPs): synthesis, characterization, and oxidative stress-mediated therapeutic actions. *Future Pharmacol* 3(1):252–295
- Ali MM, Ramadan MA, Ghazawy NA et al (2022) Photochemical effect of silver nanoparticles on flesh fly larval biological system. *Acta Histochem* 124:1–10
- Mohamad EA, Ramadan MA, Mostafa MM et al (2023) Enhancing the antibacterial effect of iron oxide and silver nanoparticles by extremely low frequency electric fields (ELF-EF) against *S. aureus*. *Electromagn Biol Med*. <https://doi.org/10.1080/15368378.2023.2208610>
- Mostafa MM, Mohamad EA, Ramadan MA et al (2022) Reduced graphene oxide @ magnetite nanocomposite and ELF-EF effect on *Staphylococcus aureus* growth inhibition. *Egypt J Chem* 66:267–278
- Amin RM, Mohamed MB, Ramadan MA et al (2009) Rapid and sensitive microplate assay for screening the effect of silver and gold nanoparticles on bacteria. *Nanomedicine* 4(6):637–643

9. Lorenzana-Vázquez G, Pavel I, Meléndez E (2023) Gold nanoparticles functionalized with 2-thiouracil for antiproliferative and photothermal therapies in breast cancer cells. *Molecules* (Basel, Switzerland) 28(11):4453
10. Mohamad EA, Rageh M, El-Aldoula RA et al (2023) Examination of the interaction between bovine albumin and gold nanoparticles. *Egypt J Chem*. <https://doi.org/10.21608/ejchem.2023.223345.8267>
11. Ramadan MA, Sharaky M, Faid AH (2022) Ionic gelation synthesis, characterization and cytotoxic evaluation of chitosan nanoparticles on different types of human cancer cell models. *Egypt J Chem* 65(2):153–159
12. Abed Shlaka W, Saeed RS (2023) Gold and silver nanoparticles with modified chitosan /PVA: synthesis, study the toxicity and anticancer activity. *Nanomed Res J* 8(3):231–245
13. Faid AH, Shouman SA, Badr YA et al (2022) Enhanced cytotoxic effect of doxorubicin conjugated gold nanoparticles on breast cancer model. *BMC Chem* 16(1):90
14. Faid AH, Shouman SA, Badr YA et al (2022) Gold nanoparticles loaded chitosan encapsulate 6-mercaptopurine as a novel nanocomposite for chemo-photothermal therapy on breast cancer. *BMC Chem* 16(1):94–94
15. Qin Z, Wang Y, Randrianalisoa J et al (2016) Quantitative comparison of photothermal heat generation between gold nanospheres and nanorods. *Sci Rep* 6(1):29836
16. Hinds DT, Belhout SA, Colavita PE et al (2023) Microsphere-supported gold nanoparticles for SERS detection of malachite green. *Mater Adv* 4(6):1481–1489
17. Faid H, Mostafa AEM, Ramadan MA (2022) Improved anticancer activity of doxorubicin gold nanohybrid on breast cell line. *Int J Adv Eng Civ Res* 2(1):36–47
18. Zou Y, Mei D, Yuan J et al (2021) Preparation, characterization, pharmacokinetic, and therapeutic potential of novel 6-mercaptopurine-loaded oral nanomedicines for acute lymphoblastic leukemia. *Int J Nanomed* 16:1127–1141
19. Flórez Barajas FJ, Sánchez Acevedo ZC, Peña Pedraza H (2019) Síntesis y caracterización de nanopartículas de oro en solución utilizando quitosán como agente reductor. *Respuestas* 24(2):49–55
20. Skehan P, Storeng R, Scudiero D et al (1990) New colorimetric cytotoxicity assay for anticancer-drug screening. *J Natl Cancer Inst* 82:1107–1112
21. Faid AH, Shouman SA, Thabet NA et al (2022) Laser enhanced combinatorial chemo-photothermal therapy of green synthesis gold nanoparticles loaded with 6mercaptopurine on breast cancer model. *J Pharm Innov* 18:144–148
22. Salim SA, Kamoun EA, Evans S et al (2021) mercaptopurine-loaded sandwiched tri-layered composed of electrospun polycaprolactone/ poly(methyl methacrylate) nanofibrous scaffolds as anticancer carrier with antimicrobial and antibiotic features: sandwich configuration nanofibers, release study and in vitro bioevaluation tests. *Int J Nanomed* 16:6937–6955
23. Brusač E, Jeličić M-L, Cvetnić M et al (2021) A comprehensive approach to compatibility testing using chromatographic, thermal and spectroscopic techniques: evaluation of potential for a monolayer fixed-dose combination of 6-mercaptopurine and folic acid. *Pharmaceuticals* 14(3):274
24. Ahmed AH, Badr YAE, Shouman SA et al (2018) Green synthesis of spherical gold nanoparticles by chitosan for 6 mercaptopurine delivery. *Arab J Nucl Sci Appl* 51(4):175–180
25. Ahmed AH, Badr YAE (2018) Improvement of 6-mercaptopurine efficiency by encapsulated in chitosan nanoparticles. *Arab J Nucl Sci Appl* 51(4):181–186
26. Huang H, Liu R, Yang J et al (2023) Gold nanoparticles: construction for drug delivery and application in cancer immunotherapy. *Pharmaceutics* 15(7):1868
27. Faid AH, Shouman SA, Badr YA et al (2022) Enhanced photothermal heating and combination therapy of gold nanoparticles on a breast cell model. *BMC Chem* 16(1):66
28. Ramadan MA, El-Tayeb TA (2023) Photostability, cytotoxicity and photothermal impact of agNPs, CoAgNC and IOAgNC on HEp-2 laryngeal carcinoma cells. *SN Appl Sci*. <https://doi.org/10.1007/s42452-023-05472-y>
29. Loutfy SA, Salaheldin TA, Ramadan MA et al (2017) Synthesis, characterization and cytotoxic evaluation of graphene oxide nanosheets. in vitro liver cancer model. *Asian Pac J Cancer Prev* 18:955–961
30. Sekar R, Basavegowda N, Thathapudi JJ et al (2023) Recent progress of gold-based nanostructures towards future emblem of photo-triggered cancer theranostics: a special focus on combinatorial phototherapies. *Pharmaceutics* 15(2):433
31. Anik MI, Mahmud N, Al-Masud A et al (2022) Gold nanoparticles (GNPs) in biomedical and clinical applications: a review. *Nano Sel* 3(4):792–828
32. Mendes R, Pedrosa P, Lima JC et al (2017) Photothermal enhancement of chemotherapy in breast cancer by visible irradiation of gold nanoparticles. *Sci Rep* 7(1):017–11491

Publisher's Note

Springer Nature remains neutral with regard to jurisdictional claims in published maps and institutional affiliations.

Submit your manuscript to a SpringerOpen[®] journal and benefit from:

- Convenient online submission
- Rigorous peer review
- Open access: articles freely available online
- High visibility within the field
- Retaining the copyright to your article

Submit your next manuscript at ► [springeropen.com](https://www.springeropen.com)